

# Supplementary Materials

## The Potential of X-ray Photoelectron Spectroscopy for Determining Interface Dipoles of Self-Assembled Monolayers

Thomas C. Taucher, and Egbert Zojer\*

Institute of Solid State Physics, Graz University of Technology, NAWI Graz, Petersgasse 16, 8010 Graz, Austria.

\*Corresponding author: [egbert.zojer@tugraz.at](mailto:egbert.zojer@tugraz.at), +43/316/873-8475

# 1 Information on the employed basis functions

The basis functions employed in the FHI-aims simulations have the format

$$\Phi(r) = \frac{u(r)}{r} * Y_{lm}(\Theta, \Phi) \quad (S1)$$

in spherical coordinates  $(r, \Theta, \Phi)$  relative to a given atomic center. FHI-aims provides for every atomic species a preconstructed *species\_defaults* file. The used tight basis sets were not further adjusted, because they afforded the required accuracy and efficiency. Note: If a higher tier for the basis set is used, i.e., when using tight settings, all lower basis functions must be included as well.

*Table S1. Basis functions that have been used for all calculations performed with FHI-aims<sup>1</sup>. The abbreviations read as follows<sup>1</sup>:  $X(nl, z)$ , where  $X$  describes the type of basis function where  $H$  stands for hydrogen-like functions and ionic for a free-ion like radial function. The parameter  $n$  stands for the main/radial quantum number,  $l$  denotes the angular momentum quantum number ( $s, p, d, f, \dots$ ), and  $z$  denotes an effective nuclear charge, which scales the radial function in the defining Coulomb potential for the hydrogen-like function. In the case of free-ion like radial functions,  $z$  specifies the onset radius of the confining potential. If *auto* is specified instead of a numerical value, the default onset is used.*

	H	C	N	S	Au
Minimal	valence(1s, 1.0)	valence(2s, 2.0) valence(2p, 2.0)	valence(2s, 2.0) valence(2p, 3.0)	valence(3s, 2.0) valence(3p, 4.0)	valence(6s, 1.0) valence(5p, 6.0) valence(5d, 10.0) valence(4f, 14.0)
First tier	H(2s, 2.1) H(2p, 3.5)	H(2p, 1.7) H(3d, 6) H(2s, 4.9)	H(2p, 1.8) H(3d, 6.8) H(3s, 5.8)	ionic(3d, auto) H(2p, 1.8) H(4f, 7.0) Ionic(3s, auto)	ionic(6p, auto) H(4f, 4.7) ionic(6s, auto) H(5g, 10.0) H(3d, 2.5)
Second tier	H(1s, 0.85) H(2p, 3.7) H(2s, 1.2) H(3d, 7.0)	H(4f, 9.8) H(3p, 5.2) H(3s, 4.3) H(5g, 14.4) H(3d, 6.2)	H(4f, 10.8) H(3p, 5.8) H(1s, 0.8) H(5g, 16.0) H(3d, 4.9)	H(4d, 6.2) H(5g, 10.8)	

<sup>1</sup> As described in the FHI-aims manual, version January 23, 2017.

## 2 A posteriori screening via an image charge model

To account for the screening of the highly polarizable metal substrate, the calculated orbital energies were corrected by the following screening contribution:

$$E_{C1s,screened}[eV] = E_{C1s}[eV] + 27.2114 \cdot \frac{1}{4 \cdot \epsilon \cdot 1.889716 \cdot (z[\text{\AA}] - z_0[\text{\AA}])} \quad (\text{S2})$$

Here,  $\epsilon$  is the dielectric constant of the SAM; in our case we chose  $\epsilon = 3.9$  according to measurements on biphenyl SAMs.<sup>2</sup> The constant  $z_0$  is the position of the image plane of the Au(111) surface, which was set to 0.9 Å above the average z-position of the top Au layer.<sup>3,4</sup> The z-position of the atom, to whose core level the screening is applied, is denoted as  $z$ . The two conversion factors, 27.2114 and 1.889716, are there to convert Hartree to eV and Bohr to Å, respectively. In passing we note that this approach neglects direct screening effects within the SAM and also the fact that the SAM is only of finite thickness. The screening shifts the calculated core levels to more negative values, i.e. smaller binding energies, and, naturally, is most relevant for the ones closest to the substrate.

## 3 The damping factor

To account for the finite escape depth of the ejected electrons<sup>5</sup>, a damping factor depending on the kinetic energy of the incident photons was applied to scale the contributions of the individual C atoms to the XP spectra. It is given by:

$$w_i(d) = w_0 \cdot e^{-\frac{d}{\lambda}} \quad (\text{S3})$$

Here  $w_i(d)$  is the scaling factor of the  $i$ -th C1s orbital. It depends on the vertical distance  $d$  between the  $i$ -th atom and the topmost Carbon atom of the SAM, and a damping factor  $\lambda$ , which is defined as  $\lambda = 0.3E_{KIN}^\beta$ . Here,  $E_{KIN}[eV]$  is the kinetic energy of the escaping electron, i.e., the difference between the energy of the incident photons and the calculated core level orbital energy of the C1s electron (set to 580 eV for this study).  $\beta$  is an empirical attenuation factor, which was set to 0.5 in accordance with previous studies on similar systems.<sup>6</sup> Finally,  $w_0$  is a scaling constant, which does not change the shape of the spectrum.

## 4 Flowchart describing the computational procedure

1

### DFT Simulation

For calculating core-level energies in the initial state a single DFT calculation of the optimized geometry is sufficient to get the orbital energies of all the core-levels.

A

### Geometry optimization

1. Start with a geometry of the system from an educated guess / experimental data of the adsorbed molecules on the metal substrate.
2. Create a suitable unit cell for applying the repeated slab approach.
3. Optimize the geometry of the system to find the geometry minimizing the total energy of the system and the forces per molecule.

B

### Core-level energies

Get the Kohn-Sham energies of all levels contributing to the spectrum.

C

### Aligning

To be able to compare different calculations, all the energies have to be aligned, e.g., to the Fermi level of each system (consistent with the experimental procedure).

2

### Screening

To account for screening by the polarizable (metal) substrate, the orbital energies have to be shifted depending on their distance to the substrate.

3

### Creating the spectrum

A

### Broadening

A Gaussian broadening is applied to the calculated core-level binding energies to produce a spectrum from the individual orbital energies.

B

### Damping

The contributions of each core-level to the overall spectrum depends on the escape depth of the photoelectron. Thus, the contribution from all core-levels are scaled depending on their distance from the SAM surface.

C

### Summing up

To create the final XP spectrum of the system associated with a specific core level (e.g., C 1s), the scaled Gaussian peaks of all relevant atoms are summed up.

## 5 Testing the hypothesis of vacuum level alignment for system VIa

In the main manuscript, system VIa (a biphenyl monolayer moved from its equilibrium position by 1 Å away from the substrate) is considered as the reference case for vacuum level alignment. This is backed by the negligible work function change of  $\sim 0.1$  eV induced by that layer. As a further test, we compared the XP spectra for that system and a system in which the biphenyl is shifted by 2 Å (system VIb). In case there was no interaction between adsorbate and substrate in VIa, there should be no change in the calculated spectra between VIa and VIb. This is indeed what we find, as shown in Figure S1.

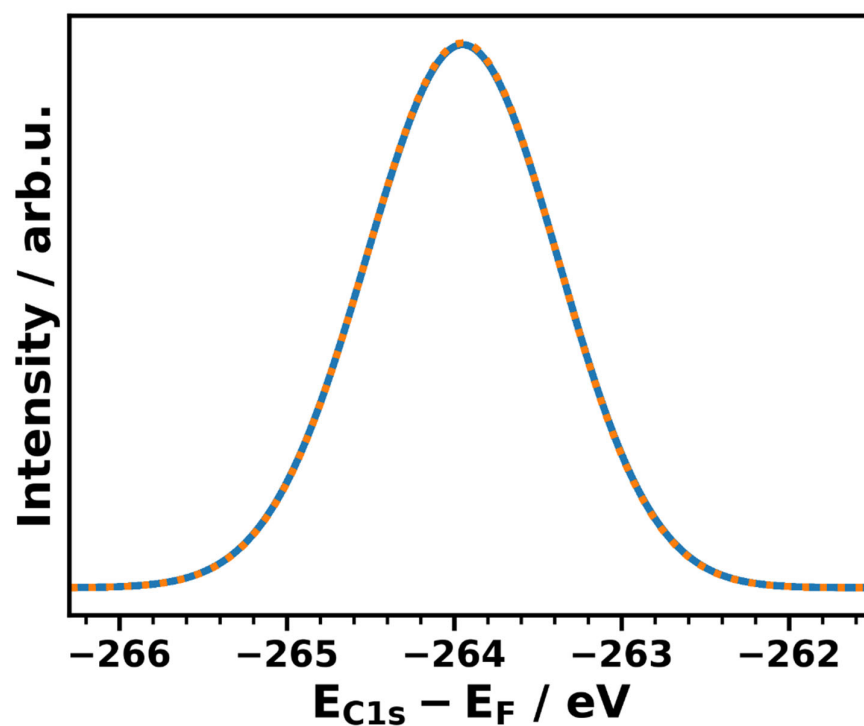


*Figure S1. Calculated XP spectra of system VIa (blue, solid line) and VIb (orange, dotted line), where the biphenyl SAM is moved farther away by 1 Å and by 2 Å, respectively.*

## 6 Calculated core-level binding energies and XP spectra for all systems at full coverage

For the sake of clarity, in Figure 3 of the main manuscript the core-level binding energies and XP spectra have been shown only for selected systems. A compilation of the results for all systems is contained in the following plot.

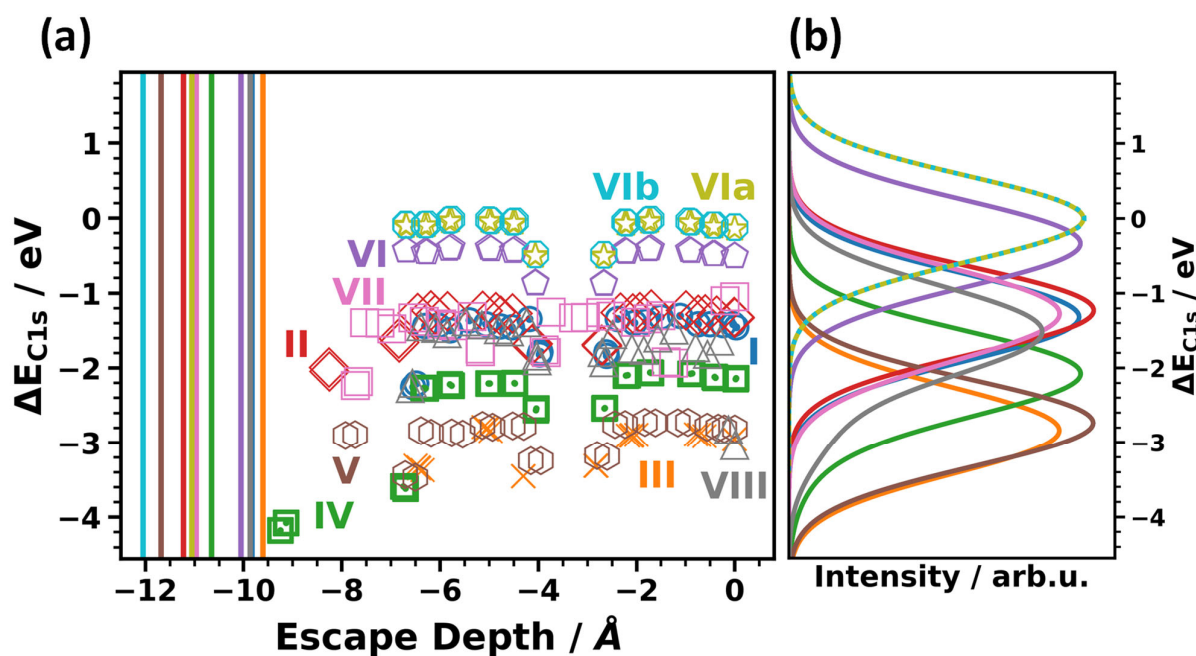


Figure S2. (a) Simulated shifts of carbon 1s orbital energies,  $\Delta E_{C1s}$ , as a function of the escape depth of the electrons for all investigated systems; (b) corresponding XP spectra generated from the calculated energy levels. The energies scale is chosen relative to the position of the peak in the XP spectrum for the vacuum-level aligned system VIa. The escape depth defined as the distance from the topmost carbon atom is chosen as the parameter on the x-axis considering that the highest atoms primarily determine the XP spectra. As the extent of the SAMs between the bottom ring and the metal substrate varies due to the different docking groups, this choice of the x-axis also largely aligns biphenyls in the different systems. Due to the different SAM thicknesses, we included vertical lines in panel (a), which designate the positions of the centers of the atoms of the topmost Au layer. The large number of data points for each system is a consequence of the two inequivalent molecules per unit cell.

## 7 Single molecule limit

To check to what degree the data for 1/16 coverage reported in the main manuscript already describe an isolated molecule on a surface, we simulated XP spectra for system I also for 1/24 and 1/30 coverage (see Figure S3). The obtained spectra essentially coincide with that for 1/16 coverage, which suggests that the “isolated molecule” case is already achieved at that coverage.

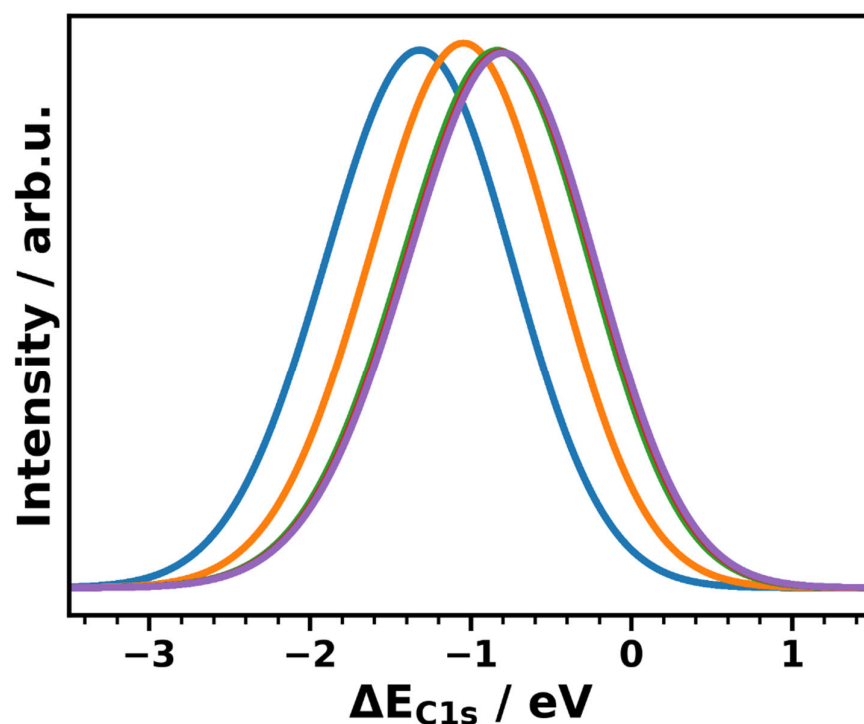


Figure S3. Calculated XP spectra of system I as a function of coverage (full coverage – blue, 1/4 coverage – orange, 1/16 coverage – green, 1/24 coverage – red, 1/30 coverage - violet). The energy scale is aligned relative to the position of the peak for the non-interacting system VIa.

## 8 Low coverage unit cells

The low coverage unit cells were created by replicating the full coverage unit cell (containing two molecules) in x- and y-direction and removing all but one molecule from the Au(111)-substrate. For a coverage of 1/4 the unit cell was duplicated only in x-direction; for the 1/16 coverage system the initial unit cell was repeated four times in x-direction and twice in y-direction; for the 1/24 cell six times in x- and twice in y-direction, and for the 1/30 coverage, this was done five times in x- and three times in y-direction.

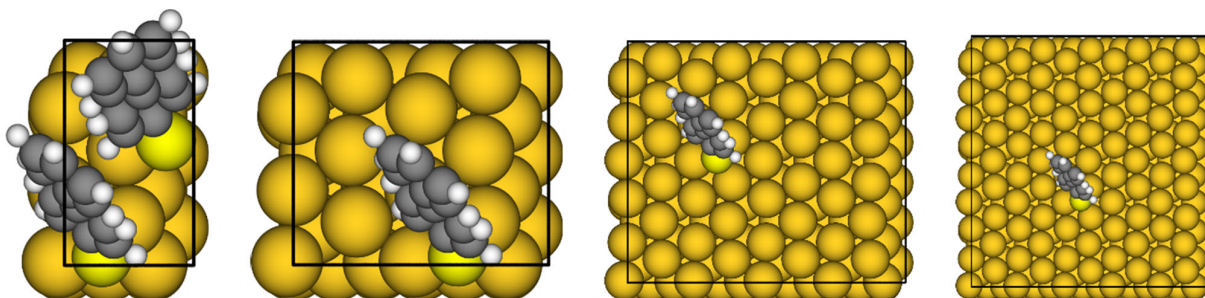
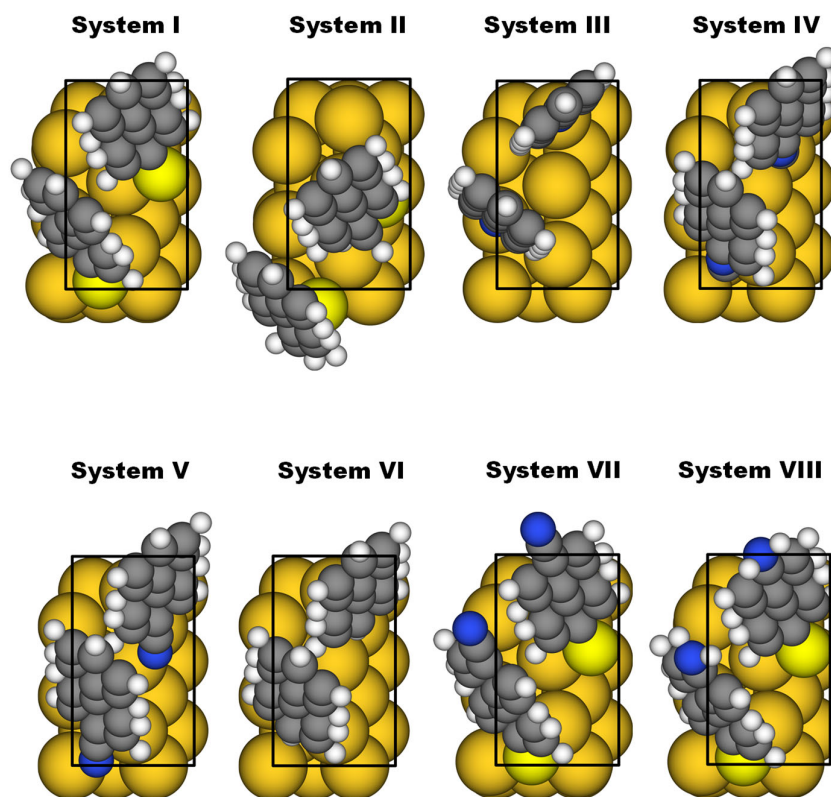


Figure S4. Top views of the unit cells for full, 1/4, 1/16, and 1/30 coverage (from left to right).

## 9 Top view of the unit cell

To be able to visually compare the tilt of each molecule in the geometrically optimized unit cell, top views of the unit cells of all systems are shown in Figure S5.



*Figure S5. Top view of the investigated systems with different docking groups bonding to the Au(111) surface slab. The tilt of the molecules is similar all systems apart from system III, where the molecules are more upright-standing.*

## 10 Plane for potential plot

To visualize the plane for which the electrostatic energy is shown in Figure 8, a top view of the (repeated) full coverage unit cell is shown in Figure S6 containing that plane.

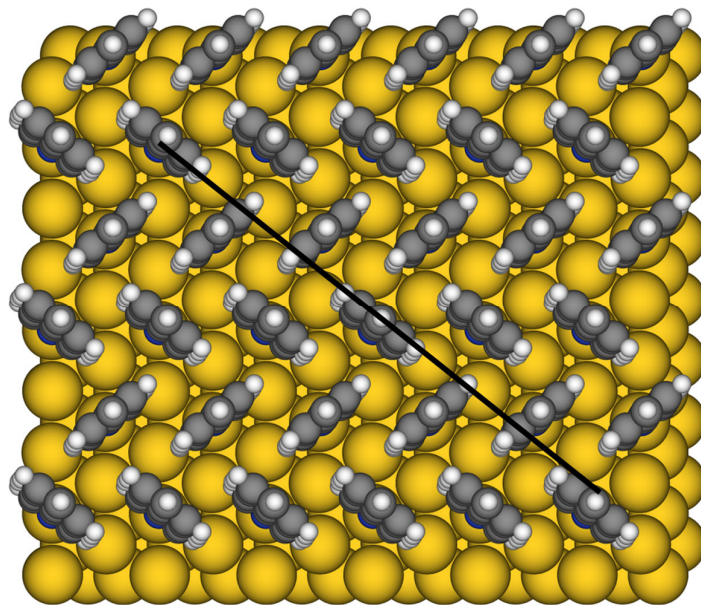


*Figure S6. Top view of system II with a black line indicating the plane used for the 2D electrostatic energy plot in Figure 8.*

## 11 References

- (1) Blum, V.; Gehrke, R.; Hanke, F.; Havu, P.; Havu, V.; Ren, X.; Reuter, K.; Scheffler, M. Ab Initio Molecular Simulations with Numeric Atom-Centered Orbitals. *Computer Physics Communications* **2009**, *180* (11), 2175–2196. <https://doi.org/10.1016/j.cpc.2009.06.022>.
- (2) Levstik, A.; Filipic, C.; Levstik, I. Dielectric Properties of Biphenyl. *J. Phys.: Condens. Matter* **1990**, *2* (13), 3031–3033. <https://doi.org/10.1088/0953-8984/2/13/012>.
- (3) Li, Y.; Lu, D.; Galli, G. Calculation of Quasi-Particle Energies of Aromatic Self-Assembled Monolayers on Au(111). *Journal of Chemical Theory and Computation* **2009**, *5* (4), 881–886. <https://doi.org/10.1021/ct800465f>.
- (4) Egger, D. A.; Liu, Z.-F.; Neaton, J. B.; Kronik, L. Reliable Energy Level Alignment at Physisorbed Molecule–Metal Interfaces from Density Functional Theory. *Nano Letters* **2015**, *15* (4), 2448–2455. <https://doi.org/10.1021/nl504863r>.
- (5) Lamont, C. L.; Wilkes, J. Attenuation Length of Electrons in Self-Assembled Monolayers of n-Alkanethiols on Gold. *Langmuir* **1999**, *15* (6), 2037–2042.
- (6) Gärtner, M.; Sauter, E.; Nascimbeni, G.; Petritz, A.; Wiesner, A.; Kind, M.; Abu-Husein, T.; Bolte, M.; Stadlober, B.; Zojer, E.; Terfort, A.; Zharnikov, M. Understanding the Properties of Tailor-Made Self-Assembled Monolayers with Embedded Dipole Moments for Interface Engineering. *J. Phys. Chem. C* **2018**, *122* (50), 28757–28774. <https://doi.org/10.1021/acs.jpcc.8b09440>.